

# Intrinsic permanent magnetic characteristics beyond $\text{Ce}_2\text{Co}_{17}$ with Ce/Co substitutions

Manish K. Kashyap,<sup>1,2</sup> Timothy A. Hackett,<sup>2,3</sup> Ed Moxley,<sup>2</sup> Sarvesh Kumar,<sup>4</sup> D. Paudyal,<sup>2</sup> and B. N. Harmon<sup>2,5</sup>

<sup>1</sup>*Department of Physics, Kurukshetra University, Kurukshetra 136119 (Haryana), INDIA*

<sup>2</sup>*Ames Laboratory, U.S. Department of Energy, Iowa State University, Ames, Iowa 50011-3020, USA*

<sup>3</sup>*Department of Biochemistry, University of Nebraska, Lincoln, Nebraska 68588-0664, USA*

<sup>4</sup>*Inter University Accelerator Centre, Aruna Asaf Ali Marg, New Delhi 110067, INDIA*

<sup>5</sup>*Department of Physics and Astronomy, Iowa State University, Ames, Iowa 50011-3160, USA*

By understanding the small easy axis magnetocrystalline anisotropy energy (MAE) of hexagonal  $\text{Ce}_2\text{Co}_{17}$ , an attempt has been made to improve anisotropy and consequently to obtain better characteristics for a high energy permanent magnet via site selective substitutional doping of Ce/Co with suitable elements. The present calculations of the electronic and magnetic properties of  $\text{Ce}_2\text{Co}_{17}$  and related substituted compounds have been performed using the full potential linear augmented plane wave (FPLAPW) method within the generalized gradient approximation (GGA). Sm-substituted compounds were simulated using Coulomb corrected GGA (GGA+ $U$ ) to provide a better representation of energy bands due to the strongly correlated Sm- $f$  electrons. The formation energies for all substituted compounds are found to be negative which indicate their structural stability. Of the substitutions, Zr substitution at the Co-dumbbell site enhances uniaxial anisotropy of  $\text{Ce}_2\text{Co}_{17}$ . Furthermore, Sm-substitution at Ce-2c sites favors incremental MAE whereas a La-substitution at both 2b- and 2c-sites depletes the tiny MAE in  $\text{Ce}_2\text{Co}_{17}$ . These observed trends in the MAE have been examined in terms of contributions from various electronic states. Finally,  $\text{Ce}_2\text{Zr}_2\text{Co}_{15}$  and  $\text{SmCeCo}_{17}$  are foreseen as suitable materials for designing permanent magnets derived from the crystal lattice structure of hexagonal  $\text{Ce}_2\text{Co}_{17}$ .

PACS numbers: 71.20.Eh, 75.50.Ww, 71.15.Mb

## I. INTRODUCTION

Permanent magnetic materials play an important role in improving the efficiency, sustainability, and performance of commercial products in electric power generation, transportation, and other energy-use sectors of the global economy. Besides a high Curie Temperature ( $T_c$ ), desirable permanent-magnets (P-Ms) must have a high energy product  $BH_{\text{max}}$  and should be cost effective.  $BH_{\text{max}}$  is related to remnant magnetization ( $M_r$ ) and coercivity ( $H_c$ ) which originate from the magnetocrystalline anisotropy energy (MAE). The MAE is one key factor for determining the easiness of a particular magnetic material to become magnetized in one direction, while being resistant to magnetization in other directions [1, 2]. The magnetic materials with high  $H_c$ , uniaxial MAE, and  $BH_{\text{max}}$  have extraordinary applications in high-tech media and ferromagnetic electrodes of spintronic devices with high magnetic-noise immunity and thermal stability. Due to economic and geopolitical issues, there is an incentive to produce P-Ms free from critical (expensive) rare earth elements. Ce-based magnets may be a prime choice in this direction due to their non-criticality, relatively low price, and the abundance of Ce [1].

Numerous experimental and theoretical efforts have been made to enhance the MAE of  $\text{Ce}_2\text{Co}_{17}$  by various means [3–7]. Streever [4] used their NMR results to evaluate the spin-orbit contribution to the magnetic anisotropy of Co atoms in  $R\text{Co}_5$  compounds. They found the easy c-axis Co anisotropy arises from the 2c sites. Ke

et al. [3] investigated the origin of MAE in doped  $\text{Ce}_2\text{Co}_{17}$  and confirmed that the dumbbell sites have a very negative contribution to the MAE in  $\text{Ce}_2\text{Co}_{17}$ , while the MAE is enhanced by replacing Co dumbbell sites with a pair of Fe or Mn atoms. X-ray diffraction (XRD) measurements [5] on magnetically aligned  $\text{Ce}_2\text{Co}_{17-x}\text{Al}_x$  powders with  $x = 0 - 3$  exhibit an easy-axis of magnetic anisotropy at room temperature. Substitution of Al for Co leads to a change of the magnetocrystalline anisotropy of the Co sublattice from the basal plane to c axis. The anisotropy increases with Al concentration ( $x$ ), goes through a maximum value of 17.7 kOe at  $x = 2$  and then decreases. Sun et al. [6] prepared  $\text{Ce}_2\text{Co}_{17-x}\text{Mn}_x$  ( $x = 0-4$ ) by arc melting in argon atmosphere and found by XRD measurements that all these magnetically aligned powered samples exhibit an easy axis magnetic anisotropy at room temperature, attaining a maximum value of 30.1 kOe at  $x = 2$ .

Sm-Co magnets are strong permanent magnets developed in the early 1960s and mainly exist in three hard magnetic phases:  $\text{SmCo}_5$ ,  $\text{SmCo}_7$ , and  $\text{Sm}_2\text{Co}_{17}$ .  $\text{Sm}_2\text{Co}_{17}$  can be derived from the  $\text{SmCo}_5$  structure and in this process, Co enrichment with respect to  $\text{SmCo}_5$  yields an increase in magnetization and  $BH_{\text{max}}$  but at a cost of the MAE [8, 9]. In a similar way, the hexagonal  $\text{Ce}_2\text{Co}_{17}$  system (2-17 series) containing four Co sublattices defined by Wyckoff sites 12k, 12j, 6g, and 4f, can also be obtained from  $\text{CeCo}_5$  (hexagonal  $\text{CaCu}_5$  structure with 191:P6/mmm space group) by replacing every third Ce atom by a pair of Co-atoms [3]. It is clear from the example of Sm magnets, 1-5 systems have better

anisotropy but low magnetization due to a small number of Co atoms. Therefore, it is preferable to work with 2-17 systems if control over decreasing MAE can be achieved.

Ke et al. [10] studied  $R(\text{Fe}_{1-x}\text{Co}_x)_{11}\text{TiZ}$  ( $R = \text{Y}$  and  $\text{Ce}$ ;  $Z = \text{H}$ ,  $\text{C}$ , and  $\text{N}$ ) systems for identifying improved magnetic properties via saturation magnetization  $M$ , Curie temperature  $T_C$ , and magnetocrystalline anisotropy energy coincident with reduction of critical materials in permanent magnets. They found the interstitial C doping significantly increases the uniaxial anisotropy in  $\text{Ce}(\text{Fe}_{1-x}\text{Co}_x)_{11}\text{Ti}$  for  $0.7 < x < 0.9$ , which may provide the best combination of all three intrinsic magnetic properties for permanent applications.  $\text{Nd}_2\text{Fe}_{14}\text{B}$ -based sintered magnets were investigated extensively and used widely since being discovered in 1984 [11, 12]. Tian et al. [13] recently discovered the practical value of  $R_2\text{Fe}_{14}\text{B}$  ( $R = \text{Pr}$ ,  $\text{Nd}$ ) magnets can be improved by proper doping of nitrogen into some interstitial sites. Ke and van Schilfgaarde [14] explained when Li is substituted by Fe in lithium nitride, the resultant compound;  $\text{Li}_2(\text{Li}_{1-x}\text{Fe}_x)\text{N}$  behaves in many aspects similar to that of rare earth element. In addition, they unveiled an analytical model to describe the magnetocrystalline anisotropy energy (MAE) in solids as a function of band filling. The MAE decomposed into a sum of transitions between occupied and unoccupied pairs. This model also yielded the MAE in good qualitative agreement with its value from first-principles calculations for  $\text{Li}_2(\text{Li}_{1-x}\text{T}_x)\text{N}$ , with  $T = \text{Mn}$ ,  $\text{Fe}$ ,  $\text{Co}$ , and  $\text{Ni}$  systems. These examples indicate doping substitutional replacement of non-critical atoms is pivotal for enhancing the MAE in particular compounds.

Pure  $\text{Ce}_2\text{Co}_{17}$  exhibits poor anisotropy characteristics and has a theoretical energy product of only 31 MGOe [15], therefore it is not a suitable P-M. Sun et al. [16] also established poor performance of  $\text{CeCo}_5$ -based compounds;  $\text{Ce}(\text{Co}_{0.73}\text{Cu}_{0.135}\text{Fe}_{0.135})_{5.35}$  and  $\text{Ce}(\text{Co}_{0.73}\text{Cu}_{0.135}\text{Fe}_{0.135})_{5.55}$  for permanent magnets due to the formation of  $\text{Ce}_2\text{Co}_{17}$  phase with  $T_C < 20^\circ\text{C}$ . Improvement in the anisotropy of  $\text{Ce}_2\text{Co}_{17}$  is expected by suitable substitution of Co as observed in the literature, perhaps to a point beyond which it is auspicious for PM fabrication. Due to the presence of inequivalent sites of the Co and Ce atoms in  $\text{Ce}_2\text{Co}_{17}$ , it may be possible to substitute these atoms by foreign atoms and design new compounds with better magnetic properties and enhanced MAE. The main aim of this study is to theoretically investigate the change in the MAE via this type of substitution. For this purpose, the full potential density functional approach has been selected for studying Co substitution by Zr/Ti, and Ce substitution by Sm/La.

## II. COMPUTATIONAL APPROACH

The base compound;  $\text{Ce}_2\text{Co}_{17}$  crystallizes in the  $\text{Th}_2\text{Ni}_{17}$ -type (space group: 194; P63/mmc) structure [17]. For spin polarized calculations of pristine  $\text{Ce}_2\text{Co}_{17}$

and its 4f site substitution, we considered the lattice parameters of  $\text{Ce}_2\text{Co}_{17}$  [8] whereas for 2b/2c substitution, we have modeled the lattice parameters as an average of lattice parameters of  $\text{Ce}_2\text{Co}_{17}$  and  $\text{Sm}_2\text{Co}_{17}$ [18]/ $\text{La}_2\text{Co}_{17}$  [19]. The calculations were performed using density functional theory (DFT) [20] based upon the full-potential linearized augmented plane wave (FPLAPW) method [21] as implemented in the WIEN2k crystal program [22]. The generalized gradient approximation (GGA) under the parameterization of Perdew-Burke-Ernzerhof (PBE) [23] was used to construct the exchange-correlation (XC) functionals for all compounds except Sm-related ones. For Sm substitutions, XC functional were considered within GGA+ $U$  to correct on-site f-electron correlation by taking  $U_{eff} = U - J = 6.0$  eV [24], which includes the Coulomb parameter,  $U = 6.7$  eV and exchange parameter  $J = 0.7$  eV for the Sm-f electrons. We used  $R_{mt}k_{max} = 8.5$  for basis functions, and the cut-off energy and charge convergence criteria were set to  $10^{-6}\text{Ry}$  and  $10^{-6}$ e, respectively, due to the sophisticated MAE calculations involved. The k-space integration was performed using the modified tetrahedron method [25]. Self-consistency was obtained using 168 k-points in the irreducible Brillouin zone (IBZ). A scalar relativistic calculation, with GGA or GGA+ $U$  formalisms, was first performed to obtain a self-consistent potential. After fixing this potential, relativistic effects were included with the second variational treatment of spin-orbit coupling [26]. The MAE stems from the orbital contribution to the magnetic moment mainly. We calculated the MAE by using the magnetic force theorem [27]. The MAE constant ( $K$ ), which is MAE/volume of the cell, is then calculated from the expression:

$$K = \sum_{j,k}^{occu} \epsilon_j(\hat{n}_2, k) - \sum_{j,k}^{occu} \epsilon_j(\hat{n}_1, k) \quad (1)$$

Here  $\epsilon_j$  is the Kohn-Sham eigenvalue evaluated for each magnetization orientation. In Eq. 1,  $j$  labels occupied states and the  $k$  is a particular  $k$ -point in the Brillouin zone,  $\hat{n}_1$  is [001], i.e.,  $c$ -axis and  $\hat{n}_2$  is taken along the [100] direction. Here, the positive/negative value of  $E$  indicates the uniaxial/easy-plane anisotropy. The calculations of MAE demand a fine energy resolution and dense mesh of in  $k$ -space, hence, we set up a  $17 \times 17 \times 15$   $k$ -point mesh for all the anisotropy calculations in the spin orbit coupling environment.

## III. RESULTS AND DISCUSSION

The identification of effective sites for substitution is needed to enhance the MAE of  $\text{Ce}_2\text{Co}_{17}$ . The literature reveals that previous researchers substituted  $\text{Co}_{4f}$  (dumbbell sites) as shown in Fig.1 by foreign elements and observed a significant change in the MAE [3, 5–7]. Along the same line, we started with similar substitution

by Ti and Zr. Further, Ce atoms in  $\text{Ce}_2\text{Co}_{17}$ , presented at  $2b$  and  $2c$  sites, as highlighted by different colors in Fig. 1, are also expected to contribute significantly, thus we also identified these sites and investigated the substitutions at these by Sm and La. The symbolic representation used for resultant alloys obtained by  $4f$ ,  $2b$  and  $2c$  site substitutions is depicted in Fig. 2. The orbital moments as obtained by proper substitutions are also mentioned to show the importance of the alloy within this figure exclusively.

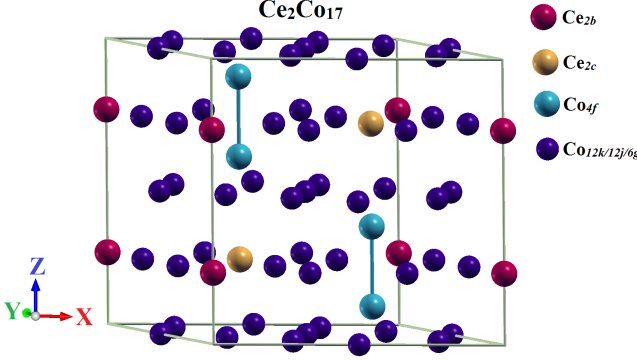


FIG. 1. Schematics for  $\text{Ce}_2\text{Co}_{17}$  showing Co dumbbell at  $4f$  sites and Co  $2c/2b$  sites, available for substitution.

In order to estimate the stability of the computed structure with respect to  $\text{Ce}_2\text{Co}_{17}$ , the formation energies;  $E_{for}$  (defined by the difference of the accumulated sum of equilibrium energies of all constituent atoms from the equilibrium energy of the resultant compound) was estimated which are depicted in the contour plot (Fig. 3). We observe that out of the studied compounds, only  $\text{Ce}_2\text{Ti}_2\text{Co}_{15}$  and  $\text{SmCeCo}_{17}$  are more stable and easy to synthesize as compared to  $\text{Ce}_2\text{Co}_{17}$ . However, all compounds are stable as verified from the negative values of formation energies which is a good indication of the feasibility of these compounds experimentally as well.

The total density of states (DOS) and atom resolved density of states at  $4f$ ,  $2b$  and  $2c$  sites in  $\text{Ce}_2\text{Co}_{17}$ ,  $\text{Ce}_2\text{Ti}_2\text{Co}_{15}$  and  $\text{Ce}_2\text{Zr}_2\text{Co}_{15}$  are depicted in Fig. 4. All three total DOS are highly spin polarized, indicating the strong magnetism in the alloys. With Ti/Zr substitution, the states for majority spin above the Fermi level ( $E_F$ ) increases due to fewer d-electrons i.e. in  $3d^2/4d^2$  configurations as compared to Co with  $3d^7$  configuration. As expected, Ce- $f$  states contribute mainly in bands above  $E_F$ . The states in the vicinity of  $E_F$  are required for electrical conductivity. The Co- $d$  states at various sites for Ti/Zr substitution in  $\text{Ce}_2\text{Co}_{17}$  are analyzed in Fig. 5. It is evident that  $d$ -DOS of Co at the  $12k$  and  $6g$  sites is not much affected by Ti/Zr substitution. A drastic change in  $d$ -DOS of Co at  $12j$  site can be identified above  $E_F$ . However, these states are located at energy greater than  $2\text{ eV}$  above  $E_F$ , so these are insignificant in the vicinity of  $E_F$  for easy excitations. Thus any change in total DOS is mainly due to the presence of Ti/Zr- $d$  states in the

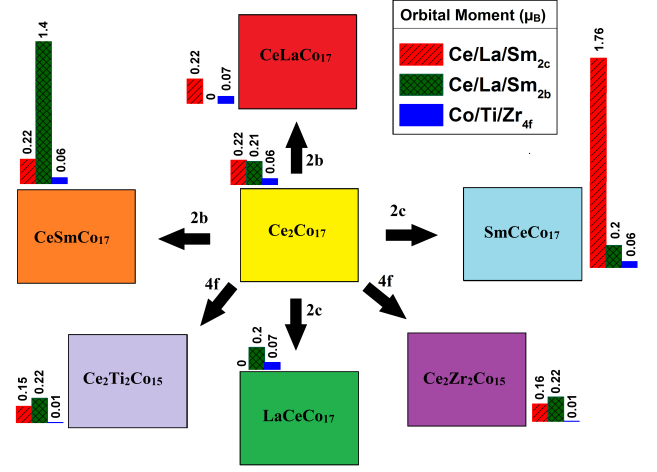


FIG. 2. Symbolic site specification and nomenclature for Ce and Co substitution in  $\text{Ce}_2\text{Co}_{17}$  at  $4f$ ,  $2b$  and  $2c$ .

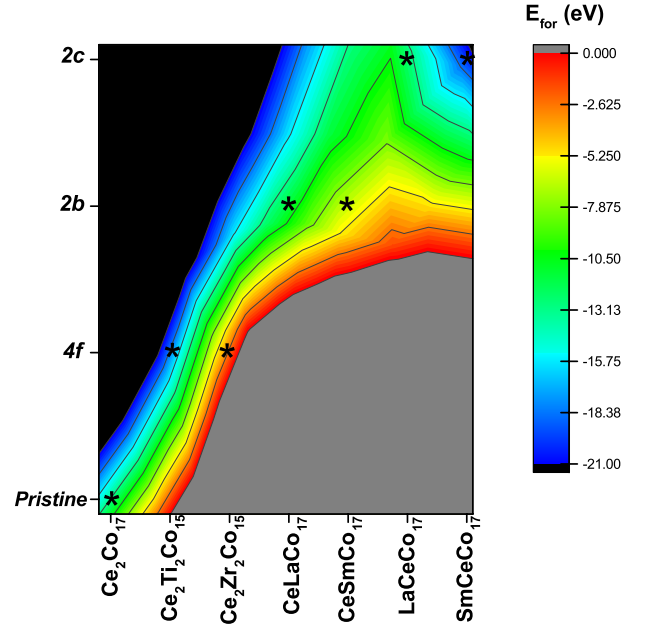


FIG. 3. The contour plot for  $E_{for}$  of the pristine  $\text{Ce}_2\text{Co}_{17}$  and  $4f/2b/2c$  substituted alloys (Here \* represents the actual magnitude of  $E_{for}$  with a particular substitution).

substituted alloys. To emphasize the significant changes in total DOS, the atom resolved DOS at the substituted Co-site is plotted with separate colors.

After identifying the effect of substitution of Co-atoms (at dumbbell sites) on the electronic properties of  $\text{Ce}_2\text{Co}_{17}$ , we have extended this study to Ce-site substitutions by Sm and La atoms. Fig. 6 depicts DOS of Ce/Sm/La- $f$  states at  $2b$  and/or  $2c$  sites. On analysis, it is found that for the DOS at the dumbbell site;  $\text{Co}_{4f}$ - $d$  remains unaffected with these substitutions. Further for substitution at  $2b$  or  $2c$  by La, the unoccupied La- $f$  are

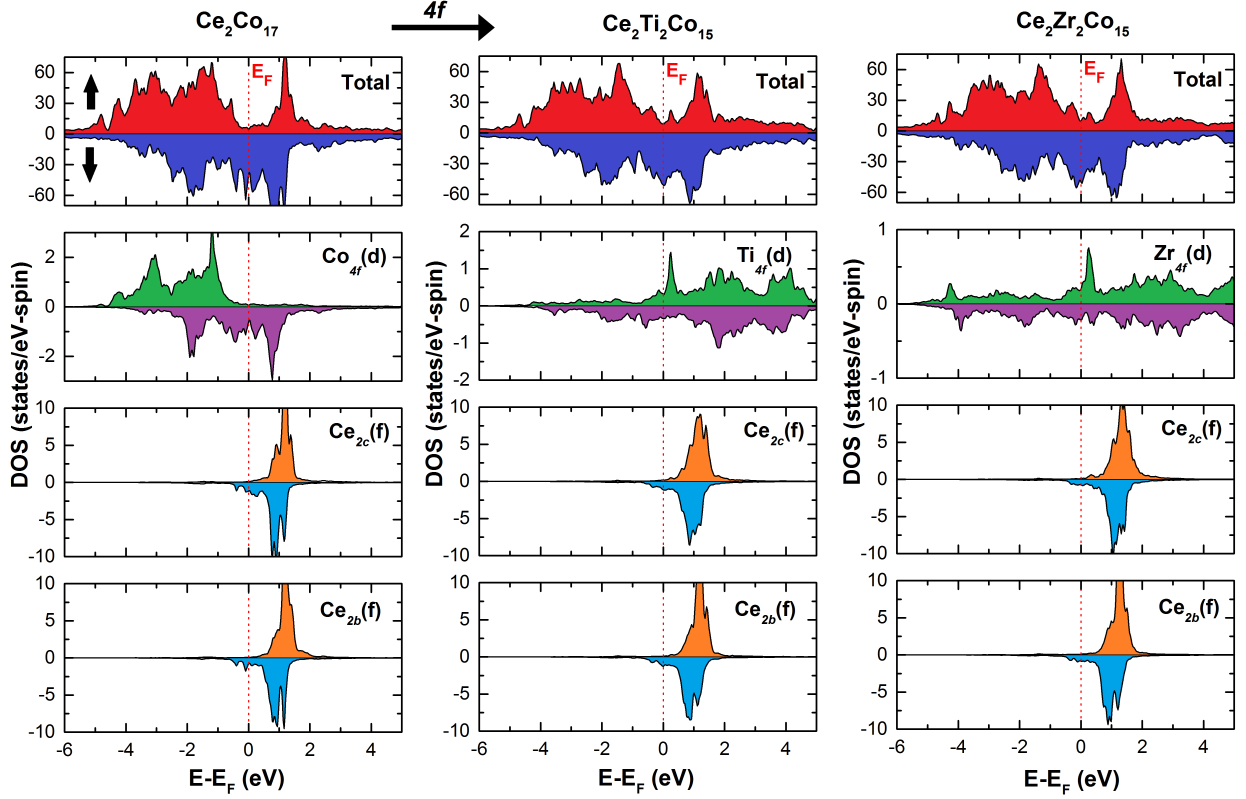


FIG. 4. Total and atom resolved DOS at 2b, 2c and 4f sites in  $\text{Ce}_2\text{Co}_{17}$ ,  $\text{Ce}_2\text{Ti}_2\text{Co}_{15}$  and  $\text{Ce}_2\text{Zr}_2\text{Co}_{15}$

unavailable in the vicinity of  $E_F$  which reduces the spin polarization in the resultant system. Significant change in total DOS is governed by Sm substitution at 2b and 2c sites. The two Sm-sites substitutions behave quite differently. While 2c substitution gives rise to more occupied Sm-f states, the 2b-substitution produces very few Sm-f DOS in the occupied region. The remaining Ce-atom in the unit cell on the other site, has similar type of DOS for both 2b/2c substitution. Further, these are found to be little perturbed compared to the case of pristine  $\text{Ce}_2\text{Co}_{17}$ . To confirm any change on Co-sites after substitution, we also analyzed all the Co sites (not shown for brevity). But surprisingly, all states are found to possess similar DOS as that of pristine case and do not have significant influence in deciding the qualitative features of total DOS. However, the strong spin polarization at each site results in better exchange spitting in all resultant alloys.

Total valence electronic charge densities,  $n(r)$  in the (110) and  $\text{Co}_{4f}$  - dumbbell planes for (i) pristine  $\text{Ce}_2\text{Co}_{17}$  (ii)  $\text{Ce}_2\text{Ti}_2\text{Co}_{15}$  (iii)  $\text{CeSmCo}_{17}$  and (iv)  $\text{SmCeCo}_{17}$  compounds were analyzed using the xcrysden program [28] to examine the effect on the neighboring atoms after substitution at 4f, 2b and 2c sites in  $\text{Ce}_2\text{Co}_{17}$ . Focusing on pristine  $\text{Ce}_2\text{Co}_{17}$  (Fig.7) the effect of symmetrical  $\text{Co}_{4f}$  atoms aligned in the dumbbell form is clearly visible, with maximum charge density along the dumbbell axis (see green color inside hexagonal contour in Fig.7 as a

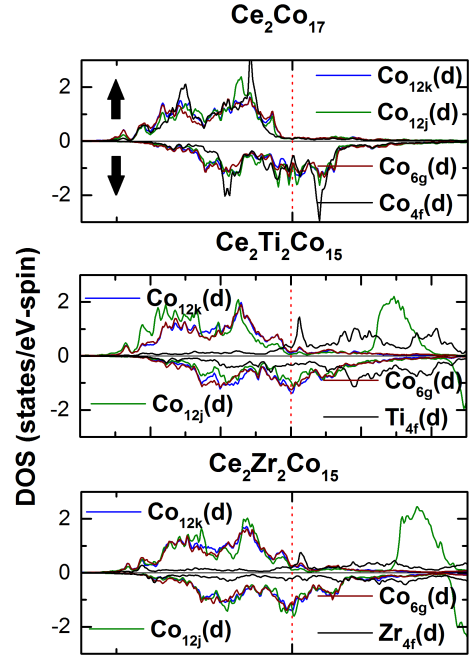


FIG. 5. Partial DOS at all types of Co-sites in  $\text{Ce}_2\text{Co}_{17}$ ,  $\text{Ce}_2\text{Ti}_2\text{Co}_{15}$ , and  $\text{Ce}_2\text{Zr}_2\text{Co}_{15}$ .

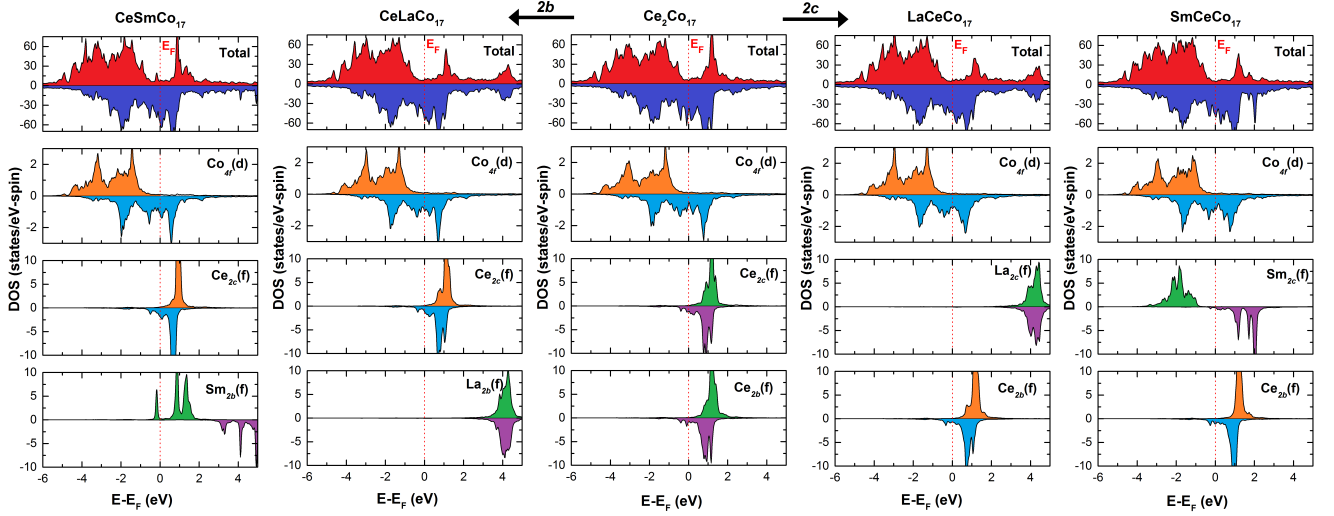


FIG. 6. Total and atom resolved DOS at  $2b$ ,  $2c$  and  $4f$  sites in  $\text{CeLaCo}_{17}$ ,  $\text{CeSmCo}_{17}$ ,  $\text{LaCeCo}_{17}$  and  $\text{SmCeCo}_{17}$

projection of charge density from two Co-atoms aligned in the dumbbell form on both sides of the (110) plane in perpendicular direction). Further charge density contours in the  $\text{Co}_{4f}$  dumbbell plane for  $\text{Ce}_2\text{Co}_{17}$  indicate that two Co atoms at  $4f$  sites are tightly bonded with each other. But the substitution of Ti in place of Co atoms at  $4f$  sites decreases the charge densities along the  $\text{Co}_{4f}$  dumbbell axis due to the presence of a lesser number of d-electrons. The dumbbell Ti-atoms are not tightly bonded and are expected to decrease the magnetism in the resultant compound.

The charge densities along the  $\text{Co}_{4f}$  dumbbell axis for Sm- $2b/2c$  substitution are again enhanced. However, in these substitutions, the effect on charge densities along  $\text{Co}_{4f}$  dumbbell plane is modest and dumbbell Co-atoms are again tightly bonded (as in case of  $\text{Ce}_2\text{Co}_{17}$ ). The substituted Sm atom behaves differently in the resultant compound which is clearly visible from the shape of Ce and Sm atoms as depicted in Fig.7(iii) and (iv), respectively. The Ce atom tends to polarize the neighboring Co-atoms but the Sm atom preserves its spherical shape. The two factors, strong bonding between dumbbell Co-atoms and spherical shape of Sm atoms seem to increase the overall magnetism. These density plots demonstrate the importance of Co-dumbbell sites in the present compounds not only for  $4f$  but also for  $2b/2c$  substitutions.

The atom resolved spin and orbital moments at each site are listed in Table-I. It is clear that  $4f$  site substitution decreases the total moment of  $\text{Ce}_2\text{Co}_{17}$  whereas  $2b/2c$  substitution increases the same. The magnetization is found to be in excellent agreement with the previous experiment [29] and calculation [3]. The Co spin moments on each site are similar  $\approx 1.5\text{-}1.8 \mu_B$ . However on  $4f$  substitution, the Ti/Zr moment aligns antiparallel to Co moment at other sites which causes a significant

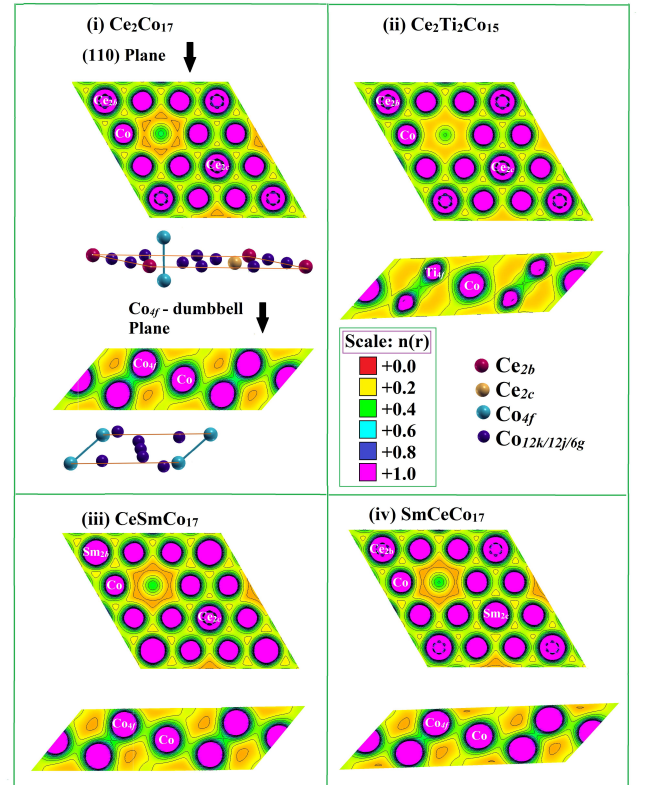


FIG. 7. Total valence electronic charge density difference,  $n(r)$  in units of  $e/\text{\AA}^3$  in  $\text{Ce}_2\text{Co}_{17}$ ,  $\text{Ce}_2\text{Ti}_2\text{Co}_{15}$ ,  $\text{CeSmCo}_{17}$  and  $\text{SmCeCo}_{17}$ .

decrease in total spin moment of the resultant alloy.

Regarding  $2b/2c$  substitution by La, the La orbital moment not only drops down to zero but also its spin mo-

TABLE I. Calculated total orbital ( $\mu_l$ ), spin ( $\mu_s$ ) and total moments ( $\mu_t$ ) in  $\mu_B$  for  $\text{Ce}_2\text{Co}_{17}$  and all related substituted compounds

Material			Magnetic moment( $\mu$ )							
			Ce(2c)	Ce(2b)	Co(12k)	Co(12j)	Co(6g)	Co(4f)	Inter.	Total
$\text{Ce}_2\text{Co}_{17}$	This work	$\mu_s$	-0.58	-0.63	1.60	1.78	1.55	1.74	-4.04	23.58
		$\mu_l$	0.22	0.21	0.08	0.09	0.07	0.06	-	1.78
		$\mu_t$	-	-	-	-	-	-	-	25.36
	Ke et al. [3]	$\mu_s$	-0.84	-0.90	1.51	1.56	1.51	1.65	-1.1	23.40
		$\mu_l$	0.38	0.42	0.10	0.11	0.08	0.07	-	2.43
		$\mu_t$	-	-	-	-	-	-	-	25.8
Expt [29]		$\mu_t$	-	-	-	-	-	-	-	25.4
$\text{Ce}_2\text{Zr}_2\text{Co}_{15}$ Zr (4f)	This work	$\mu_s$	-0.47	-0.52	1.22	1.34	1.07	-0.19	-3.36	15.52
		$\mu_l$	0.20	0.47	0.07	0.10	0.08	0.01	-	1.95
		$\mu_t$	-	-	-	-	-	-	-	16.37
$\text{Ce}_2\text{Ti}_2\text{Co}_{15}$ Ti (4f)	This work	$\mu_s$	-0.58	-0.66	1.27	1.92	1.16	-0.52	-4.22	16.07
		$\mu_l$	0.15	0.22	0.07	0.10	0.07	0.01	-	1.62
		$\mu_t$	-	-	-	-	-	-	-	17.69
$\text{CeLaCo}_{17}$ La (2b)	This work	$\mu_s$	-0.62	-0.12	1.67	1.56	1.63	1.81	-4.12	25.18
		$\mu_l$	0.22	0.00	0.09	0.12	0.08	0.07	-	1.86
		$\mu_t$	-	-	-	-	-	-	-	27.04
$\text{CeSmCo}_{17}$ Sm (2b)	This work	$\mu_s$	-0.60	4.82	1.65	1.55	1.60	1.77	-3.44	30.08
		$\mu_l$	0.22	-1.40	0.09	0.11	0.08	0.06	-	0.38
		$\mu_t$	-0.48	3.42	1.74	1.66	1.68	1.83	-3.44	30.46
$\text{LaCeCo}_{17}$ La (2c)	This work	$\mu_s$	-0.11	-0.67	1.67	1.56	1.63	1.81	-4.18	25.09
		$\mu_l$	0.00	0.20	0.08	0.10	0.08	0.07	-	1.66
		$\mu_t$	-	-	-	-	-	-	-	26.75
$\text{SmCeCo}_{17}$ Sm (2c)	This work	$\mu_s$	5.02	-0.66	1.66	1.56	1.63	1.79	-3.32	30.56
		$\mu_l$	-1.76	0.20	0.08	0.11	0.08	0.06	-	-0.06
		$\mu_t$	3.26	-	-	-	-	-	-	30.50

ment gets reduced. There is not much change either in orbital or in spin moment observed for Ce as well as Co atoms. However, this La-substitution slightly increases the total moment due to dilution of antiparallel alignment of La and Co spin moments. On the other hand, a significant change is observed for Ce substitution by Sm in  $\text{Ce}_2\text{Co}_{17}$ . The Sm atom with  $4f^5$  configuration has the ability to enhance the total moment. The large increase in total magnetic moment is the consequence of the enhanced net Sm moment of 3.42/3.26  $\mu_B$  at 2b/2c sites in  $\text{CeSmCo}_{17}$ / $\text{SmCeCo}_{17}$ . Furthermore, the Sm moment aligns antiparallel/parallel to the Ce/Co spin moment which also favors the increase in total moment. Focusing on orbital moment only, we have observed that all atoms have very small orbital moments except for Sm-atoms in  $\text{CeSmCo}_{17}$  and  $\text{SmCeCo}_{17}$  which is expected due to Sm- $4f^5$  states.

Finally, to establish the potential of the studied alloys in permanent magnets, the MAE ( $K$ ) for the studied

systems were examined in Fig.8. The value of  $K$  for  $\text{Ce}_2\text{Co}_{17}$  is poor ( $\approx 0.03 \text{ MJ/m}^3$ ) as confirmed from our calculations and there is no scope to fabricate permanent magnets based on pristine  $\text{Ce}_2\text{Co}_{17}$  alone. Further the previous calculations by Ke et al. [3] and experimental work by Hu et al. [29] also reported a tiny value (0.09  $\text{MJ/m}^3$  and 0.32  $\text{MJ/m}^3$ , respectively) of the same. The 4f- site substitution by Zr increases the MAE of  $\text{Ce}_2\text{Co}_{17}$  significantly. We found the MAE for this substitution ( $\text{Ce}_2\text{Zr}_2\text{Co}_{15}$ ) as 1.15  $\text{MJ/m}^3$  which is within reasonable agreement with the corresponding experimental value of 2.57  $\text{MJ/m}^3$  [7] and close to that predicted by Ke et. al. [3]. The substituted Zr-atom contributes positively in the value of MAE which strains alignment of the magnetization from all atoms along any other magnetic field direction except for the easy c-axis direction. In one experiment with a similar type of substitution, Al atoms in  $\text{Ce}_2\text{Al}_2\text{Co}_{15}$  [5] were found to prefer the dumbbell sites and are responsible in increasing uniaxial anisotropy—



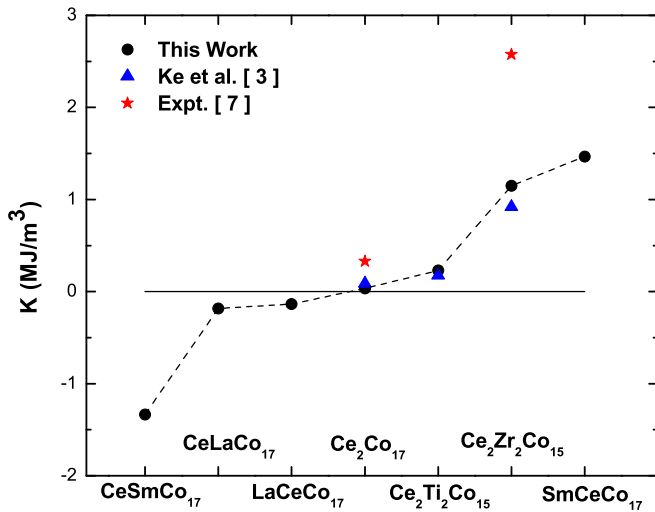


FIG. 8. Calculated MAE ( $\text{MJ}/\text{m}^3$ ) for  $\text{Ce}_2\text{Co}_{17}$  and all other substituted alloys. The corresponding experimental [7] and predicted [3] values are also presented for comparison.

which also agrees with our findings. On the other hand, the increase in MAE via similar substitution by Ti is not as effective and leads to an increase in  $K$  to  $0.23 \text{ MJ}/\text{m}^3$ . The difference in MAE obtained is a consequence of the atomic size of the substituted atom (Zr/Ti). Whereas Zr with a larger radius at dumbbell sites leads to strong hybridization; Ti-atom with smaller size than Co results in an ineffective coupling.

The site substitution at  $2b/2c$  sites by La has an opposite effect on the MAE. Rather than increasing the uniaxial anisotropy, La-substitution brings out in-plane anisotropy of the material due to the unavailability of La- $4f$  electrons. In contrast to La, site selective Sm substitution which is rich in  $f$ -electrons, can have a considerable effect on the overall MAE of the resultant compound, depending upon the crystal environment in the vicinity of substitution. In  $2b$  substitution, Sm atoms are found away from Co-dumbbell sites and have impact along  $xy$  plane, therefore, this substitution also brings down the anisotropy of  $\text{Ce}_2\text{Co}_{17}$  in planner mode. However, for  $2c$  substitution, Sm atoms align coaxially with the Co-dumbbells and thus the spin alignment along the  $c$ -axis (which is also an easy axis) is favourable. As a result, the

involvement of  $4f^5$  states gives rise to increased magnetic anisotropy in this case and the final value of  $K$  reaches to  $1.4 \text{ MJ}/\text{m}^3$ .

#### IV. CONCLUSION

In the regime of density functional theory, pristine  $\text{Ce}_2\text{Co}_{17}$  and compounds with site substitution of Ce/Co atom by La, Sm/Ti, Zr have been investigated. The Co-dumbbell sites are very crucial for the overall MAE in the resultant compound. The calculated MAE is found meaningful for Zr/Sm substitution at the  $4f/2c$  site. The enhancement of MAE in these calculations for Zr-substitution is in accordance with the available experimental data. The high convergence was cross-checked so that these results can be used as a benchmark in future experiments/calculations. Sm substitution at the  $2c$  site is vital on the basis of magnetization as well as MAE obtained. Further experimental analysis is required to establish the candidature of  $\text{Ce}_2\text{Zr}_2\text{Co}_{15}$  and  $\text{SmCeCo}_{17}$  as permanent magnets. Keeping in mind the cost of Sm, the present analysis is important as most of the prominent permanent magnets are made from  $\text{SmCo}_5$  and  $\text{Sm}_2\text{Co}_{17}$ . Therefore reducing significant content of Sm by substituting cheaper Ce in the material and preserving a large magnetic moment may open up new avenues for the development of permanent magnets at a significant reduced cost.

#### V. ACKNOWLEDGMENTS

M.K.K. would like to acknowledge UGC, New Delhi for providing Raman Post-Doctoral Fellowship vide grant No. 5-147/2016 (IC). This research is supported by the Critical Materials Institute, an Energy Innovation Hub funded by the U.S. Department of Energy (US-DoE), Office of Energy Efficiency and Renewable Energy, Advanced Manufacturing Office. The Ames Laboratory is operated for the US-DoE by Iowa State University of Science and Technology under Contract No. DE-AC02-07CH11358. T.A.H. is grateful to the US-DoE for the assistantship and opportunity to participate in the SULI program for undergraduate research.

[1] J. F. Herbst, J. J. Croat, and W. B. Yelon, *Journal of Applied Physics* **57**, 4086 (1985).  
[2] J. F. Herbst, J. J. Croat, F. E. Pinkerton, and W. B. Yelon, *Phys. Rev. B* **29**, 4176 (1984).  
[3] L. Ke, D. A. Kukusta, and D. D. Johnson, *Phys. Rev. B* **94**, 144429 (2016); ArXiv: **1610.02767**, v2 (2018).  
[4] R. L. Streever, *Phys. Rev. B* **19**, 2704 (1979).  
[5] B. gen Shen, J. yun Wang, H. wei Zhang, S. ying Zhang, Z. a Cheng, B. Liang, W. shan Zhan, and C. Lin, *Journal of Applied Physics* **85**, 4666 (1999).

[6] Z. gang Sun, S. ying Zhang, H. wei Zhang, J. yun Wang, and B. gen Shen, *Journal of Physics: Condensed Matter* **12**, 2495 (2000).  
[7] H. Fujii, M. V. Satyanarayana, and W. E. Wallace, *Journal of Applied Physics* **53**, 2371 (1982).  
[8] O. Gutfleisch, *Journal of Physics D: Applied Physics* **33**, R157 (2000).  
[9] P. Larson and I. I. Mazin, *Phys. Rev. B* **69**, 012404 (2004).

- [10] L. Ke and D. D. Johnson, Phys. Rev. B **94**, 024423 (2016).
- [11] M. Sagawa, S. Fujimura, N. Togawa, H. Yamamoto, and Y. Matsuura, Journal of Applied Physics **55**, 2083 (1984).
- [12] J. J. Croat, J. F. Herbst, R. W. Lee, and F. E. Pinkerton, Journal of Applied Physics **55**, 2078 (1984).
- [13] G. Tian, L. Zha, W. Yang, G. Qiao, C. Wang, Y. Yang, and J. Yang, AIP Advances **8**, 056207 (2018).
- [14] L. Ke and M. van Schilfgaarde, Phys. Rev. B **92**, 014423 (2015).
- [15] A. E. Ray and K. J. Strnat, "Tech. rep." (U.S. Air Force Syst. Command, Air Force Mater. Lab., 1972) p. 67.
- [16] W. Sun, K.-k. Song, M.-g. Zhu, Y.-k. Fang, N.-j. Yu, S. Wang, and W. Li, Journal of Superconductivity and Novel Magnetism (2017).
- [17] Y. Khan, Acta Crystallographica Section B **29**, 2502 (1973).
- [18] K. Buschow and A. V. D. Goot, Journal of the Less Common Metals **14**, 323 (1968).
- [19] H. Chang, N. Chen, J. Liang, and G. Rao, The European Physical Journal B - Condensed Matter and Complex Systems **33**, 55 (2003).
- [20] M. Weinert, E. Wimmer, and A. J. Freeman, Phys. Rev. B **26**, 4571 (1982).
- [21] G. K. H. Madsen, P. Blaha, K. Schwarz, E. Sjöstedt, and L. Nordström, Phys. Rev. B **64**, 195134 (2001).
- [22] P. Blaha, K. Schwarz, G. K. H. Madsen, D. Kvasnicka, and J. Luitz, *WIEN2K, An Augmented Plane Wave + Local Orbitals Program for Calculating Crystal Properties* (Karlheinz Schwarz, Techn. Universität Wien, Austria, 2001).
- [23] J. P. Perdew, K. Burke, and M. Ernzerhof, Phys. Rev. Lett. **77**, 3865 (1996).
- [24] V. I. Anisimov, F. Aryasetiawan, and A. I. Lichtenstein, Journal of Physics: Condensed Matter **9**, 767 (1997).
- [25] P. E. Blöchl, O. Jepsen, and O. K. Andersen, Phys. Rev. B **49**, 16223 (1994).
- [26] D. D. Koelling and B. N. Harmon, Journal of Physics C: Solid State Physics **10**, 3107 (1977).
- [27] A. Mackintosh and O. Andersen, "Electrons at the fermi surface," (Cambridge University Press, Cambridge, England, 1980).
- [28] A. Kokalj, Computational Materials Science **28**, 155 (2003), proceedings of the Symposium on Software Development for Process and Materials Design.
- [29] S. Hu, X. Wei, D. Zeng, X. Kou, Z. Liu, E. Brck, J. Klaasse, F. de Boer, and K. Buschow, Journal of Alloys and Compounds **283**, 83 (1999).